JOURNAL OF AIRCRAFT
Vol. 46, No. 6, November–December 2009

Active Control of Smart Fin Model for Aircraft Buffeting Load Alleviation Applications

Yong Chen*
National Research Council Canada, Ottawa, Ontario K1A 0R6, Canada
Fatma Demet Ulker†
Carleton University, Ottawa, Ontario K1S 5B6, Canada
Volkan Nalbantoglu‡
Middle East Technical University, 06531 Ankara, Turkey
Viresh Wickramasinghe* and David Zimcik*
National Research Council Canada, K1A 0R6, Canada
and
Yavuz Yaman‡
Middle East Technical University, 06531 Ankara, Turkey

DOI: 10.2514/1.42489

Following the program to test a hybrid actuation system for high-agility aircraft buffeting load alleviation on the full-scale F/A-18 vertical fin structure, an investigation has been performed to understand the aerodynamic effects of high-speed vortical flows on the dynamic characteristics of vertical fin structures. Extensive wind-tunnel tests have been conducted on a scaled model fin integrated with piezoelectric actuators and accelerometers to measure the aft-tip vibration responses under various freestream and vortical airflow conditions. Test results demonstrated that the airflow induced considerable damping to the fin structure, which generally increased with airflow speed as well as the vertical fin angle of attack relative to the airflow direction. Moreover, it was observed that at the angle of attack of 10 deg, the high-speed airflow introduced large deflection to the smart fin structure and caused significant frequency shift to the vibration modes due to nonlinear geometrical coupling of bending and torsional modes. These aerodynamic effects may adversely affect the performance and robustness of the closed-loop control laws developed based on vertical fin dynamic model identified without considering the varying aerodynamic effects. To explore this problem, the structured singular values synthesis technique was adopted to develop robust control law using smart fin model identified without aerodynamic excitations, and the aerodynamic effects on the fin structure were assumed as smart fin parametric and dynamic uncertainties. The effectiveness and robust performance of the control law was demonstrated through extensive closed-loop wind-tunnel tests using various airflow conditions. This provided a verified control law design strategy for future flight tests of the full-scale aircraft buffeting load alleviation system.

Nomenclature

D	=	vortex generator cross-sectional dimension, m
f	=	peak vortical airflow frequency, Hz
f_M	=	vortical airflow frequency in the wind tunnel, Hz
K	=	fin model ratio
k	=	Strouhal number
V	=	airflow speed, m/s
V_M	=	airflow speed in the wind tunnel, m/s
u_1	=	input to group 1, V
u_2	=	input to group 2, V
y_1	=	aft-tip acceleration, g
y_2	=	front-mid acceleration, g

Introduction

IN THE development of high-agility fighter aircraft, new designs such as leading-edge extensions (LEX), blended wing and fuselage configurations, and canards are introduced to generate strong leading-edge vortices during high angle-of-attack (AOA) maneuvers. The additional lift generated by the vortices can increase the maximum AOA during maneuvers and extend the flight envelope to the stall and poststall regime [1]. However, the vortices break at very high angles of attack and interact with the aircraft empennage, which may cause severe vibration problems to the fin structure known as buffeting [2]. Under the circumstances, the vortices emanating from the leading edge of the LEX, fuselage, or canards burst upstream of the empennage and cause extremely high-energy turbulent flows downstream to impinge on the fin structures of the aircraft. The intense and unsteady buffeting aerodynamic loads are characterized by a broadband spectrum with narrowband peak distributions. As a result, the lower vibration modes of the vertical tail are excited and introduce significant high-level dynamic stresses to the fin and empennage structures. Prolonged exposure to the buffeting loads usually leads to premature fatigue damage to the vertical fin skin and stub structures, reducing mission availability of the aircraft and increasing maintenance cost of the fleet.

The vertical fin buffeting problem affects aircraft with both twin vertical fin and single vertical fin configurations [3]. However, it is a difficult task to design fighter aircraft fin structures to withstand the intense buffeting loads. Many approaches have been investigated to alleviate the buffeting damage on the vertical fins. The flow control approach modified the vortical flowfields to reduce the intensity of the buffeting loads on the vertical fin. Rigid fences or vents have been installed to the F/A-18 LEX to create a second unsteady vortex that interacts with the vortices created by the leading-edge extension to disperse the vortices before they impinge on the vertical fin [4]. However, this modification provided limited reduction of buffet loads and was effective only at a specific range of flight conditions along with the weight and aerodynamic penalties. Moreover, the

Received 1 December 2008; accepted for publication 4 August 2009.

*Institute for Aerospace Research.
†Department of Mechanical and Aerospace Engineering.
‡Department of Aerospace Engineering.

additional vortices generated by the fence may break down at certain angles of attack, leading to more turbulent wakes [5]. On the other hand, the structural modification approach tries to strengthen the load-carrying structures of the vertical fins. For example, the stiffness of the F-15 vertical fin structure was increased by using composite brackets, thicker skin, and spars [6], but this can sometimes lead to changes in dynamic response frequency with aeroelastic implications. Multiple L-shaped brackets were added to the F/A-18 vertical tail root to provide increased structural strength. However, these modifications not only resulted in a considerable increase in structural weight, but also transferred the dynamic loads to the empennage and increased potential damage to structural components elsewhere.

An innovative smart structure-based active buffeting load alleviation system on a full-scale F/A-18 vertical fin was successfully demonstrated under the Technical Cooperative Program (TTCP) [7–11]. However, several technical issues remained outstanding that have to be investigated further. In the full-scale ground vibration test phase of this TTCP project, two mechanical shakers were used to provide simulated aerodynamic buffeting loads. The attached mechanical shakers also introduced significantly higher damping to the active vertical fin due to the heavy inertial masses of the shaker armature. This increased fin damping required higher actuation authority from the hybrid actuation system, which prohibited an accurate simulation of the buffeting load alleviation tasks and underestimated the vibration reduction performance that the hybrid actuation system could have achieved on full-scale aircraft structures. Therefore, it is desirable to evaluate the buffeting load alleviation performances using realistic aerodynamic buffeting loads.

Because of the limitation of buffeting load simulation using two mechanical shakers, the simulated aerodynamic load spectra focused mainly on two separate frequency bands to cover the major vibration modes [9]. Only two load cases were synthesized based on flight-test data to reflect the buffeting load levels at various flight conditions, namely the maximum fin response case and maximum fin damage case. However, it is important to note that simulated buffet load spectra used in the ground closed-loop experiments were statistically stationary. They were not able to reflect the transient or rapid changing aerodynamic conditions to which the vertical fins may be exposed during aircraft maneuvers in flight. Although the control laws demonstrated satisfactory performance to alleviate fin vibration responses in the ground test phase, the robustness of the control laws are yet to be evaluated using actual vortical airflows and various airflow speeds.

To investigate the technical limitations of the full-scale ground vibration test under the TTCP project, a scaled smart fin model was investigated to explore these technical challenges, specifically the impact of aerodynamic vortical loads on the dynamics of the smart fin model. Based on the knowledge of smart fin dynamics, the robustness of a closed-loop control law was evaluated using vortical aerodynamic airflows through extensive closed-loop control experiments in the wind tunnel.

Dynamic Modeling of Smart Fin Structure

Smart Fin Dynamics

The scaled smart fin model was made of a thin aluminum plate, as shown in Fig. 1. The fin structure was designed to match the first bending and first torsional modes of the F/A-18 vertical fin. A total of 24 piezoelectrictransducer (PZT) patches were bonded symmetrically to both fin surfaces to serve as strain actuators, with 12 on each side. These actuators were configured into two groups and controlled with out-of-phase voltages on either side to provide actuation authorities to the first bending and torsional modes, respectively. The material properties of the aluminum fin plate and piezoelectric patch actuators are listed in Table 1.

To understand the dynamics of the smart fin model and the impacts of aerodynamic loads on the dynamic properties of the smart fin vibration modes, experimental modal tests were conducted on the smart fin structure using the LMS Test.Lab modal analysis system. The nodal grid and modal shapes of the smart fin are shown in Fig. 2. A Brüel and Kjær impact hammer equipped with a PCB force

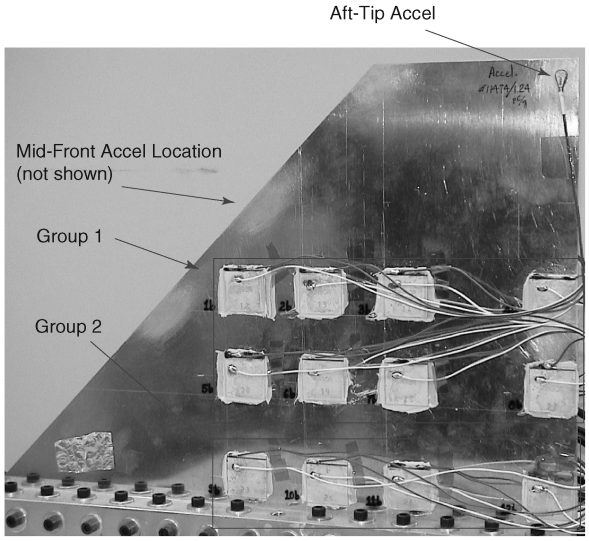

Fig. 1 Smart fin model.

transducer was used to excite the fin modes at the root. Seven miniature PCB accelerometers were used to measure the modal responses. Modal analysis results revealed four vibration modes below 150 Hz, two bending modes at 18 and 81 Hz, and two torsional modes at 50 and 121 Hz. The modal parameters are shown in Table 2.

Smart Fin Model Dynamics in Aerodynamic Environment

To investigate the impacts of vortical airflows on the smart fin dynamic properties when exposed to high-speed aerodynamic environment, extensive vibration tests were conducted in the 0.9 m × 0.9 m low-speed pilot wind tunnel of the Institute for Aerospace Research of the National Research Council Canada (NRCC). The smart fin model was clamped to a heavy base fixture at the root. This clamping condition was representative of the full-scale fin that is fastened to the fuselage through five stubs at the root. The effect of the continuous vs discrete attachment at the root was not deemed to affect the modal response of the fin. Test conditions included manually setting the smart fin model at 0 and 10 deg angle-of-attacks relative to the airflow direction. For freestream airflows, the wind speed in the wind tunnel was set at 10, 20, 30, 40, and 45 m/s, respectively, to simulate various airflow conditions. To better simulate the buffeting conditions for the smart fin model, unsteady vortical airflows were generated by vortex shedding from a square tube fixed 1.2 m upstream of the fin model in the wind tunnel. With this approach, the peak frequency of the buffeting load spectrum f_M can be determined as

$$f_M = k\frac{V_M}{D} \tag{1}$$

where V_M is the airflow speed within the wind tunnel, D is the cross-sectional dimension of the vortex generator, and k is the Strouhal number determined experimentally as 0.9. The experimental configuration is shown in Fig. 3.

For buffeting load simulation, the test conditions can be determined using basic similarity parameters

$$f = K \times f_M \times \frac{V}{V_M} \tag{2}$$

Table 1 Material properties of smart fin structure

Property	Aluminum 2024-T3	PZT BM500
Density, Kg/m^3	2796	7650
Elastic module, MPa	73.0	64.5
Thermal expansion, μm°C	23.2	——
Thickness, mm	1.02	0.50
Piezoelectric constant, $d_{31}[pC/N]$	——	175

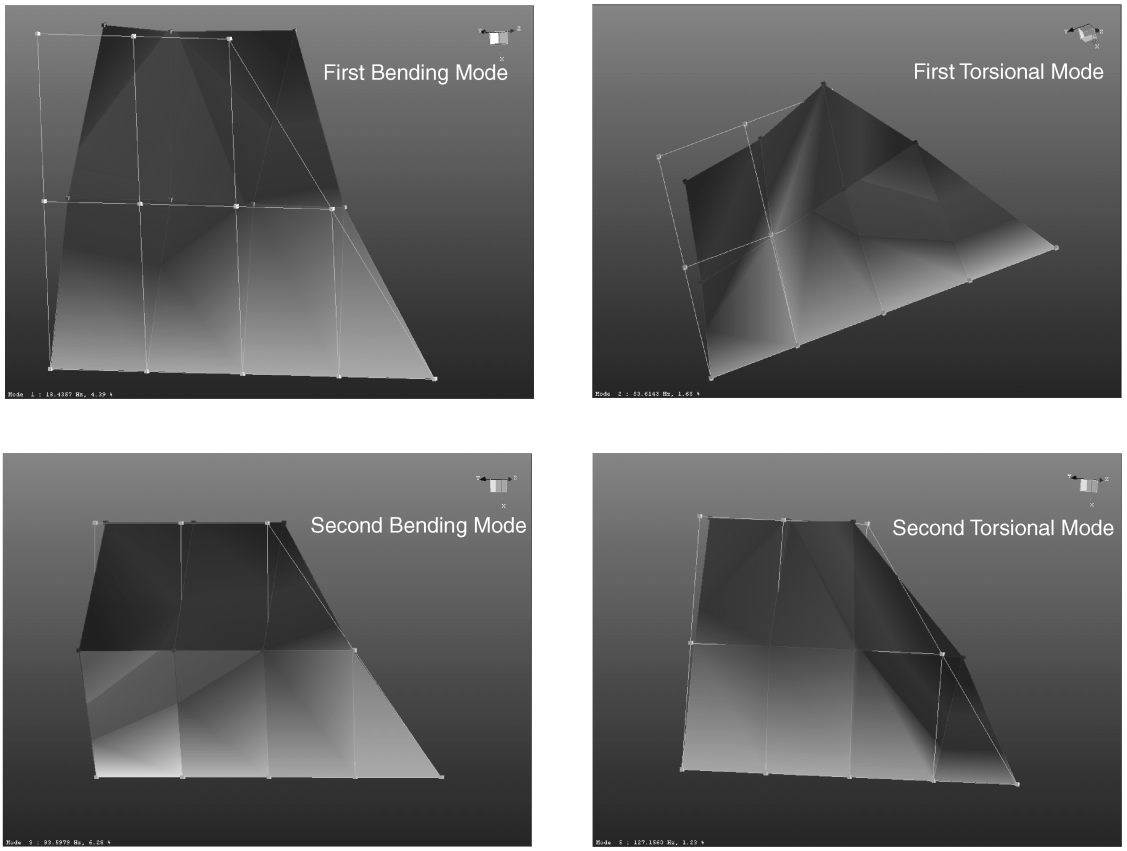

Fig. 2 Modal shapes of the smart fin model.

where f is the peak vortical airflow frequency of the buffeting loads, K is the ratio of the fin model dimensions relative to the full-scale vertical fin, and V is the vortical airflow speed to which the full-scale vertical fin structure is exposed during flight maneuvers [1]. As noted previously, the model fin was designed to match the first bending and torsional modal frequencies of the F-18 vertical fin structure. By measuring the model scale, the vortical airflow speed during flight maneuvers can be conveniently simulated by adjusting the airflow speed of the low-speed wind tunnel. Vibration amplitudes were established by the size and location of the vortex generator to ensure that large deflections (6–7 times the thickness of the fin) were induced but that the piezo wafer actuators were not overstressed in this configuration, which may have resulted in cracking. The previous TTCP project had established the capability of piezo actuators to reduce the amplitude sufficiently, and the object of this test was to establish the robustness of the control algorithm in actual airflows.

The vibration responses of the smart fin model were measured at freestream and vortical airflow conditions in the wind tunnel. The information was used to estimate the variation of the smart fin modal damping ratio and modal frequencies due to the aerodynamic loads at various airflow speeds. The test was repeated at 0 and 10 deg AOA at the yaw direction to simulate various flight conditions.

In the open-loop characterization test two accelerometers were used: one attached to the aft tip and the other to the front-mid location of the smart fin model, which were identified as critical response locations. The aft-tip acceleration responses at 0 deg AOA are shown in Fig. 4. Clearly there was a low-level broadband turbulence in the freestream airflow that was able to excite the first four modes of the fin. It was also observed that the aft-tip acceleration levels increased with the airflow speed indicating a higher level of broadband turbulence with higher airflow speed. The freestream airflow also introduced considerable aerodynamic damping to the fin structure.

To experimentally identify the smart fin modal parameters at various airflow speeds, a 60 Vpp sinusoidal signal that swept linearly from 0 to 100 Hz was applied to a TREK power amplifier to drive the 12 PZT actuator pairs. Both the sinusoidal sweep voltage input and accelerometer responses were recorded using a Nicolet vision data acquisition system. The data were postanalyzed to determine the smart fin frequency responses functions (FRFs) at various airflow conditions. The identified modal parameters were analyzed to evaluate the variation of the smart fin dynamics due to aerodynamic effects.

The FRFs revealed that the damping ratio of all vibration modes increased significantly with airflow speed. For example, the damping ratio of the first bending mode was 0.47% when tested without

Table 2 Variation of smart fin modal parameters under free airflows

Airflow condition			First bending		First torsion		Second bending	
	AOA, deg	Air speed, m/s	Frequency, Hz	Damping ratio	Frequency, Hz	Damping ratio	Frequency, Hz	Damping ratio
Freestream airflow condition	0	0	16.6	0.47%	51.0	1.36%	81.0	1.16%
		10	16.4	1.83%	49.3	1.77%	80.1	1.68%
		20	16.6	1.67%	48.6	1.79%	78.9	1.83%
		30	16.8	1.75%	48.3	2.37%	78.9	1.95%
	10	10	16.6	2.90%	48.9	1.73%	77.9	1.58%
		20	16.3	6.10%	47.7	1.86%	76.6	1.86%
		30	16.1	6.52%	47.6	2.91%	76.4	2.32%

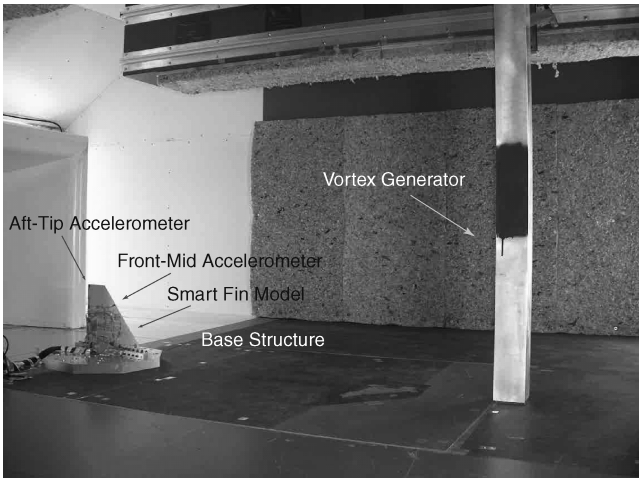

Fig. 3 Smart fin wind-tunnel test configuration.

airflow. It increased to 1.75% when exposed to 30 m/s freestream airflow disturbances. Similarly the damping ratio of the second bending mode at 81 Hz increased from 1.16 to 1.95%. The frequencies of the first torsion and second bending modes exhibited a defined shift to higher frequencies due to the excitation of airflow. Although it is expected that a similar shift in frequency should have been seen with the first bending mode, the amplitude of this shift was not sufficient to clearly overcome the measurement tolerances making this shift hard to define. The second bending mode shifted with airflow speed from 81 Hz at 0 m/s to 78.9 Hz at 30 m/s. Details of the modal parameter variation with airflow speed are listed in Table 2.

To further investigate the aerodynamic impacts on the smart fin modal parameters, the test was repeated at various free airflow speeds with a 10 deg AOA configuration. The corresponding smart fin aft-tip vibration responses are shown in Fig. 5. It was clearly shown that the modal frequencies reduced at 10 deg AOA configuration when compared with 0 deg AOA at comparable air speeds. The frequencies of higher vibration modes shifted more significantly than the lower modes and the relative frequency shift became more prominent with an increase in airflow speed. For example, when tested with 10 deg of AOA, the frequency of the second bending mode was observed as 81 Hz at 0 m/s and 77.9 Hz at 10 m/s. However, it reduced to 76.4 Hz at 30 m/s.

The smart fin aft-tip acceleration responses were also measured under vortical airflow disturbances, as shown in Fig. 6. As noted previously, there was a low-level broadband turbulence in the freestream airflow that was able to excite the first four modes of the fin. However, the addition of the vortex generator into the airflow specifically increased the vortical flow as expected but also increased the broadband turbulence in the airflow to excite all of the four modes to higher levels. The result was that not only was the amplitude of deflection of the first mode increased by 3 orders of magnitude, but

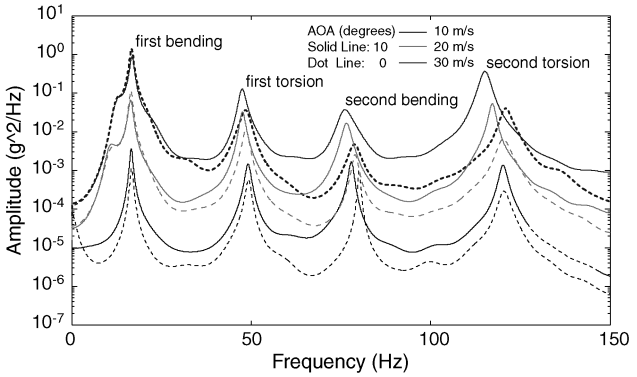

Fig. 5 Fin aft-tip responses under free airflow.

the amplitude of the other three modes also increased significantly. Because of the much higher amplitude measured, the maximum airflow speed was limited to 15 m/s during the test to avoid the piezoelectric ceramic actuator from fracture under severe fin vibration conditions. As shown in Fig. 6, the peak buffeting frequency of the vortical airflow was 9.8 Hz at 10 m/s and increased to 12.9 Hz at 15 m/s. Similar to the cases of freestream airflow, the increased airflow speed introduced higher aerodynamic damping ratio to the smart fin modes. The modal frequencies of the smart fin also reduced with the increase of AOA from 0 to 10 deg and the effect was more significant to higher vibration modes. Detailed modal parameters are listed in Table 3.

The open-loop wind-tunnel tests verified that aerodynamic loads introduced additional damping and caused modal frequency shift to the smart fin model. The extent of the influence increased with airflow speed, and the impact of vortical airflow was more significant than the freestream airflow because of the high buffeting energy intensity. Increased AOA was more critical due to the impact of additional aerodynamic loads on the smart fin surface. Referencing relevant research results [12], the shift of smart fin modal frequencies was believed to be introduced by the coupling of aerodynamic loads with smart fin geometrical nonlinearities in deformation. The aerodynamic loads applied on the smart fin surface introduced considerable deflection of the relatively flexible fin structure, especially at higher AOA configurations. The large deformation caused structural couplings between the torsional and bending modes and resulted in modal frequency shift of the smart fin dynamics. However, more dedicated investigation is necessary to identify the full nature of this aeroelastic phenomenon.

It is very important to model the structural dynamic characteristics of aircraft vertical fins when subjected to aerodynamic buffeting loads. Unfortunately, this is still a difficult task in designing vertical fin buffeting load alleviation systems. In this investigation, despite the unclear nature of this aeroelastic interaction effect, the observations on the model fin dynamics did raise a major technical concern, that is, the performance and robustness of control laws developed based on vertical fin dynamics without considering

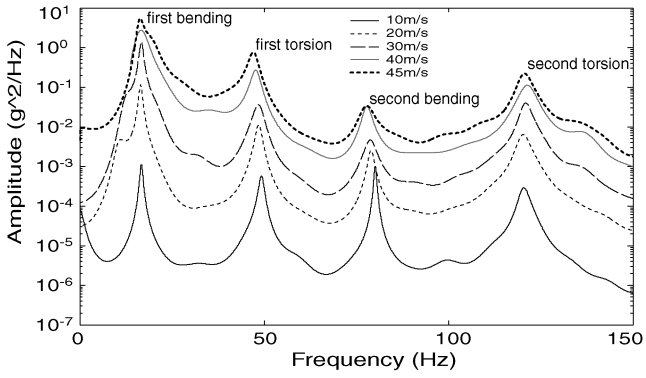

Fig. 4 Fin aft-tip responses at free airflow speeds (AOA = 0).

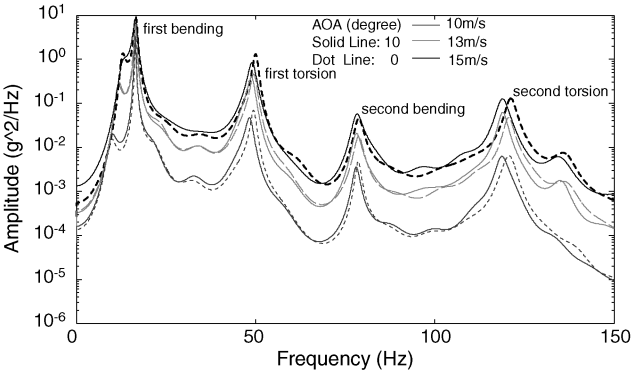

Fig. 6 Fin aft-tip responses under vortical airflow.

Table 3 Variation of smart fin modal parameters under vortical buffeting airflows

Air flow condition			First bending		First torsion		Second bending	
	AOA, deg	Air speed, m/s	Frequency, Hz	Damping ratio	Frequency, Hz	Damping ratio	Frequency, Hz	Damping ratio
Vortical airflow condition	0	0	16.6	0.47%	51.0	1.36%	81.0	1.16%
		10	16.6	2.00%	48.1	1.77%	77.4	1.30%
		13	16.6	2.31%	48.6	1.80%	77.9	1.42%
		15	16.6	2.42%	49.3	1.78%	77.5	1.53%
	10	10	16.3	2.71%	48.3	1.86%	77.1	1.51%
		13	16.3	3.03%	48.6	1.89%	77.1	1.68%
		15	16.3	2.68%	48.8	1.86%	77.0	1.75%

aerodynamic effects may degrade in realistic aircraft maneuver flight conditions. Therefore, the influences of vortical airflows on the dynamic properties of full-scale aircraft vertical fin structures should be further evaluated and the control laws should be designed based on robust criteria to account for aeroelastic uncertainties of the vertical fin dynamic properties.

Development of Robust Control Law

Robust Control Law

H_∞ synthesis technique was used to design control laws for the smart fin model. This technique can describe modeling errors and dynamic uncertainties in a framework consistent with the performance objectives. The resulting control laws are tradeoffs between robustness and performance corresponding to the model uncertainties [13]. In this investigation, the modeling errors in identification of the smart fin dynamics and the variations of the smart fin dynamics due to the airflow aerodynamics were accounted for as parametric uncertainties of the damping ratio and frequencies of each mode. The control objective was to suppress the three vibration modes below 100 Hz whereas higher structural modes beyond 100 Hz were assumed as unmodeled structural dynamics. Both the parametric and dynamic uncertainties were formulated as an additive uncertainty block and represented with linear fractional transformations. The control law performance and robustness were evaluated through extensive closed-loop experiments using various airflow speeds and vortical flow conditions.

In the closed-loop wind-tunnel test, the 12 PZT actuator pairs were divided into two groups: four bottom pairs were configured as group one to control the bending modes, and the remaining eight PZT pairs were connected as group two to control the torsional modes. Both the aft-tip and front-mid accelerometers were used as error sensors to monitor the smart fin overall vibration responses. Therefore, a two-input–two-output control system was created for the smart fin buffeting load alleviation experiments.

A block diagram formulation for the smart fin buffeting load alleviation is show in Fig. 7. The smart fin model was experimentally identified in the laboratory without airflow excitations. The block Wdist represented the dynamics of aerodynamic disturbances. The block Wnoise was a diagonal matrix that represented the measurement noise from the two accelerometers. In this investigation, both diagonal elements were selected as 5%, assuming a signal-to-noise ratio of 20. The block Wact was a diagonal matrix to penalize the actuator control voltages. Both diagonal elements were selected as 0.01 to scale the maximum control voltage on the PZT actuators to ± 100 V. The unmodeled dynamics of the smart fin model, including the nonlinearities of the aeroelastic coupling effect, were accounted for in the control process via an additive uncertainty weighting block, Wadd, defined relative to the nominal smart fin dynamic model. This frequency domain function also represented the unmodeled smart fin dynamics beyond 100 Hz, including the unmodeled second torsional mode and other higher structural vibration modes. The magnitude of additive uncertainty function was selected to vary with the frequency range of interest. A performance weight function block, Wperf, was introduced to focus the control objective on the three selected vibration modes below 100 Hz.

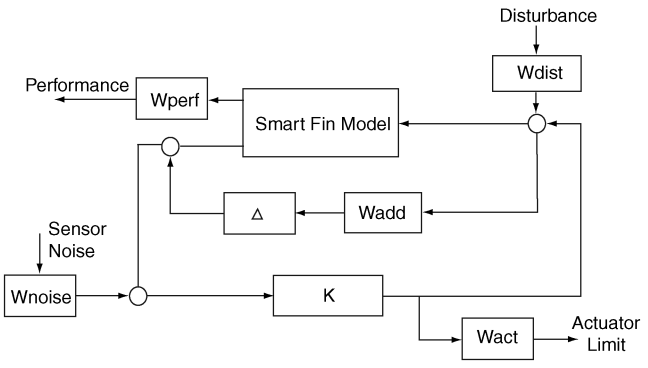

Fig. 7 Block diagram formulation of robust control law.

Control Law Implementation

The nominal FRF of the smart fin model was obtained through experimental identification without aerodynamic disturbances. The nonlinear model fin dynamics due to aeroelastic coupling was treated as a time-varying linear system, and the parametric variation of the linear system was included in the bounded additive uncertainty block. Two separate sinusoidal signals that swept linearly from 0 to 100 Hz at a rate of 1.5 Hz/s were applied to the two actuator groups, respectively. This frequency range was selected to cover the three major vibration modes, and higher vibration modes beyond 100 Hz, including the second torsional mode at 121 Hz, were assumed as unknown structural dynamics and not identified, as discussed previously. To avoid frequency interferences between the two control groups, one signal was swept upward and the other reversely. The MATLAB® system identification toolbox was used to curve-fit the time domain input and output signals and obtain a state-space representation of the smart fin model as shown in Fig. 8, where u_1 and u_2 represented the input to group 1 and group 2, and output y_1 and y_2 represented the responses of aft-tip and midaccelerometers, respectively.

The two-input–two-output control law was developed using the structured singular values synthesis technique [14] and implemented on the MATLAB® xPC TargetBox platform, which allowed rapid algorithm prototyping and hardware-in-the-loop experiments. The executable code was generated from the Simulink block diagram directly and then transferred to the target computer to run in real-time mode. A sampling rate of 500 Hz was used in the implementation. The calculated control outputs were applied to the two PZT actuator groups through the TREK 50/750 power amplifier.

Closed-Loop Experiments in Wind Tunnel

Test of Control Laws Without Considering Smart Fin Aerodynamic Effects

Closed-loop experiments were also conducted in the NRCC low-speed pilot wind tunnel. The experimental configuration of the smart fin model for buffeting load alleviation was kept the same as the open-loop identification process, as shown in Fig. 3.

Based on the transfer functions of the smart fin model identified without aerodynamic excitations, a two-input–two-output linear quadratic Gaussian (LQG) control law was developed and tested to verify the performance and robustness under various freestream

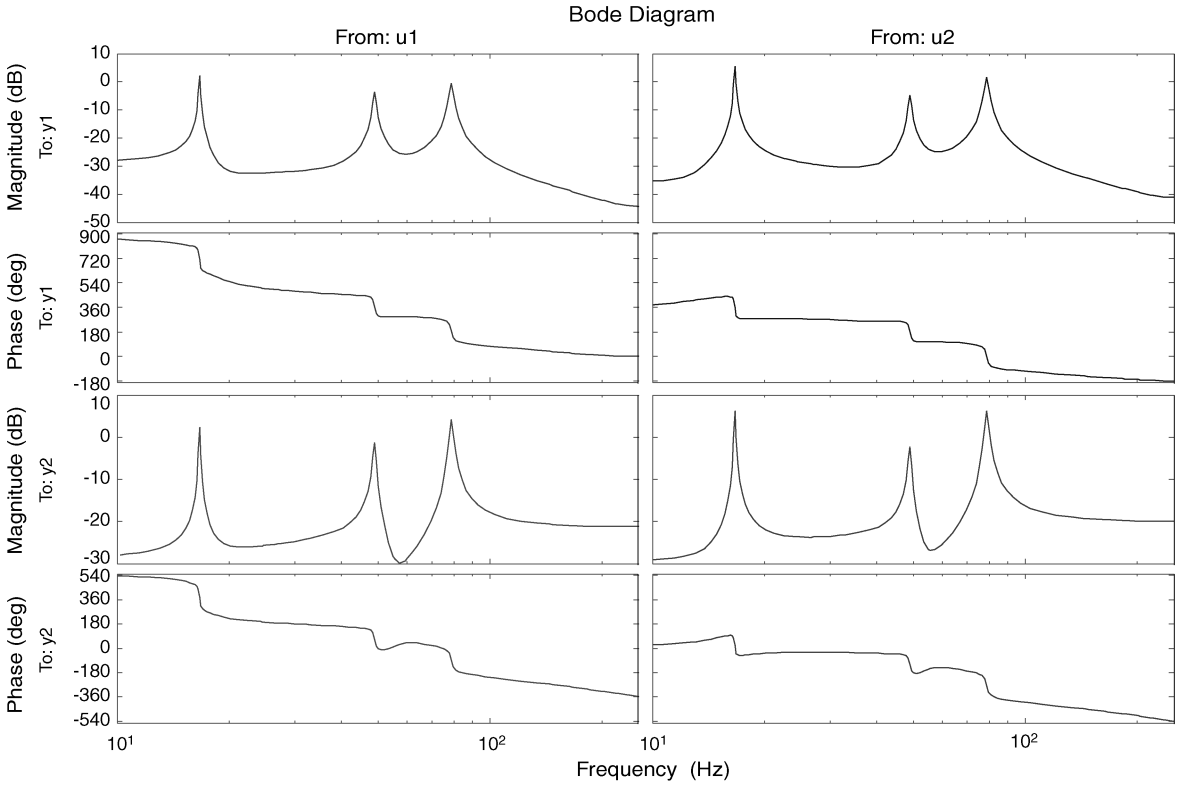

Fig. 8 Multi-input/multi-output FRFs of the smart fin model.

airflow conditions for comparing purposes with the robust control law. Test results revealed that the LQG functioned well at AOA of 0 deg, but poorly at AOA of 10 deg due to the aeroelastic coupling effect caused by the aerodynamic airflows. Typical results are shown in Fig. 9.

As shown in Fig. 9a, at 0 deg AOA the LQG control demonstrated effective suppression of all three targeted vibration modes in all tested airflow speeds. At 10 m/s, the reduction to first bending mode, first torsional mode, and second bending mode was 13.3, 7.5, and 28.7 dB, respectively. With the airflow speed increased to 30 m/s, the suppression achieved reduced to 10.0, 7.2, and 14.9 dB accordingly. No obvious control spillover was observed. The degraded vibration control performance at 30 m/s compared with 10 m/s was caused by the control authority limitation of the PZT actuators because the maximum control voltage was limited to 100 V peak in this investigation.

As shown in Table 2, the aeroelastic interaction caused significant modal frequency shift to the first torsion and second bending modes in the AOA of 10 deg configuration. At the airflow speed of 10 m/s, the LQG control law demonstrated limited robust performance by reducing control gain. It remained effective in suppressing the targeted vibration modes despite the minor modal frequency shift due to the aerodynamic flow. However, the modal frequencies of the smart fin modes, especially the second bending mode, shifted significantly at airflow speed above 20 m/s. Because the LQG control law was developed based on the smart fin dynamic model identified without aerodynamic excitations, considerable spillover was observed at the second bending mode around 81 Hz in the closed-loop control test. This test clearly demonstrated that control laws should be refined to account for the aerodynamic effects on fin structural dynamics to ensure closed-loop stability for aircraft buffeting load alleviation applications.

Test of Control Law Based on Robust Performance

Control Results with Freestream Airflow

As previously noted, a two-input–two-output control law was developed using the H_∞ synthesis technique to suppress the three

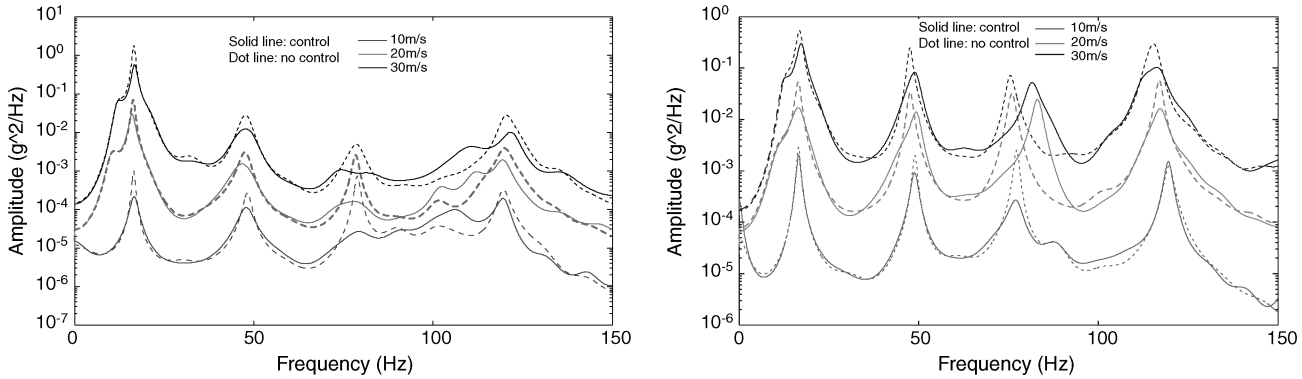

a) Control results at AOA of 0 degree **b) Control results at AOA of 10 degree**

Fig. 9 LQG control results under free airflow conditions.

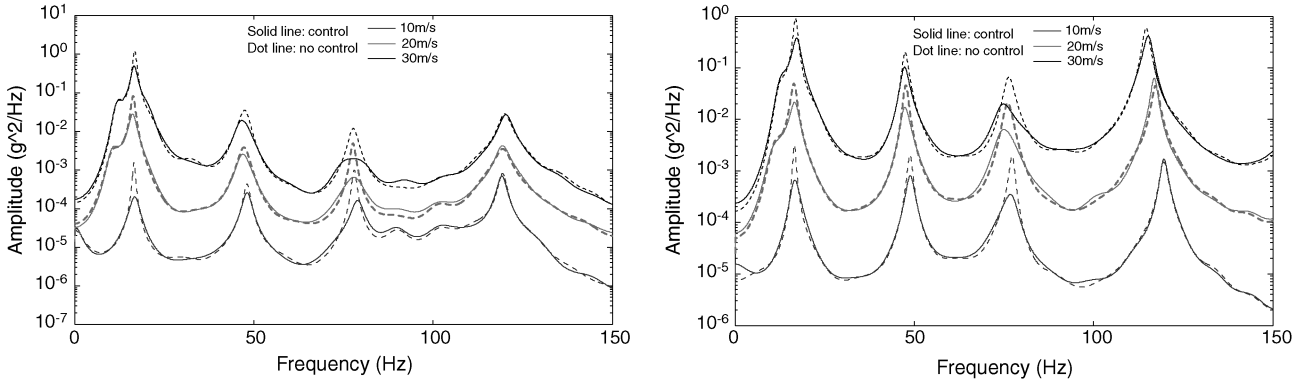

a) Control results at AOA of 0 degree **b) Control results at AOA of 10 degree**

Fig. 10 Robust control law performance under free airflow conditions.

major vibration modes below 100 Hz. The control law was tested with the same airflow conditions in the wind tunnel to compare with the LQG control law. Typical vibration control results under free airflow conditions are shown in Fig. 10.

As shown in Fig. 10, the robust control law demonstrated effective vibration reduction to all three targeted vibration modes. At the airflow speed of 10 m/s, the reduction to first bending mode, first torsional mode, and second bending mode was 17.7, 4.4, and 15.7 dB, respectively. With the airflow speed increased to 30 m/s, the achieved suppression reduced slightly to 7.7, 5.3, and 15.8 dB. The achieved overall vibration reduction was generally comparable with the LQG control law. More important, no obvious control spillover was observed beyond 100 Hz at either 0 or 10 deg AOA configurations. This not only verified the effectiveness of the proposed control law to alleviate smart fin buffeting load responses, but also demonstrated that the proposed control law development strategy was able to account for the unmodeled smart fin dynamics beyond 100 Hz as well as the modal frequency shift and variation of smart fin damping ratio due to airflow disturbances.

Control Results with Vortical Airflow

The control law performance was also verified with vortical airflows. Typical vortical buffeting load alleviation results are shown in Fig. 11.

With the configuration of 0 deg AOA, the rms value of the smart fin aft-tip response was 0.094 *g*when tested at 10 m/s free airflow condition. The rms value showed 1.35 *g* at the vortical airflow speed of 10 m/s, a dramatic increase of 23.1 dB. Comparing the smart fin responses under freestream and vortical airflow conditions, it was clearly shown that the intense buffeting load energy within the vortical airflow caused significantly higher acceleration levels to the smart fin structure. However, due to the narrow airflow speed range tested, no significant modal frequency shift or damping ratio variation of the smart fin dynamics was identified from 10–15 m/s.

The control law based on the structured singular values synthesis technique demonstrated effective vibration reduction performance and remained stable under both AOA configurations. With the increase of airflow speed the achieved vibration suppression to the three targeted smart fin modes decreased due to the intense buffeting energy related to the vortical airflows. At the AOA of 10 deg and airflow speed of 10 m/s, the first bending mode at 16.3 Hz was suppressed by 16.2 dB, the first torsional mode at 48 Hz was suppressed by 4.3 dB, and the second bending mode at 77 Hz was reduced by 19.7 dB. At the airflow speed of 15 m/s, suppression to the three vibration modes reduced to 7.2, 5.0, and 8.3 dB, respectively. No obvious control spillover was observed throughout the experiment.

This observation also demonstrated that the dramatic increase of buffeting energy required the PZT actuators to provide higher actuation force accordingly for effective buffeting load alleviation performance. However, the maximum control voltage was limited to 100 V in this experiment. Therefore, the limited actuation authority was not able to maintain a constant vibration reduction performance throughout the vortical buffeting load control experiment. This test verified that an efficient, compact, yet powerful actuation system is essential to high-agility fighter aircraft for effective buffeting load alleviation applications.

Control Results with Variable Airflow

To further verify the control law performance under unstationary vortical airflow speed conditions, variable airflow speed was generated in the wind tunnel. This was achieved by adjusting the

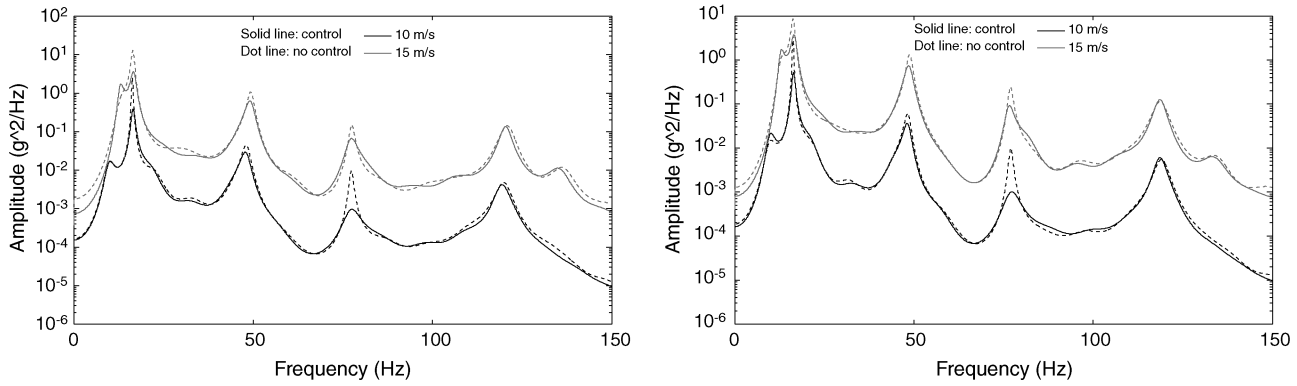

a) Control results at AOA of 0 degree **b) Control results at AOA of 10 degree**

Fig. 11 Robust control law performance under vortical airflow conditions.

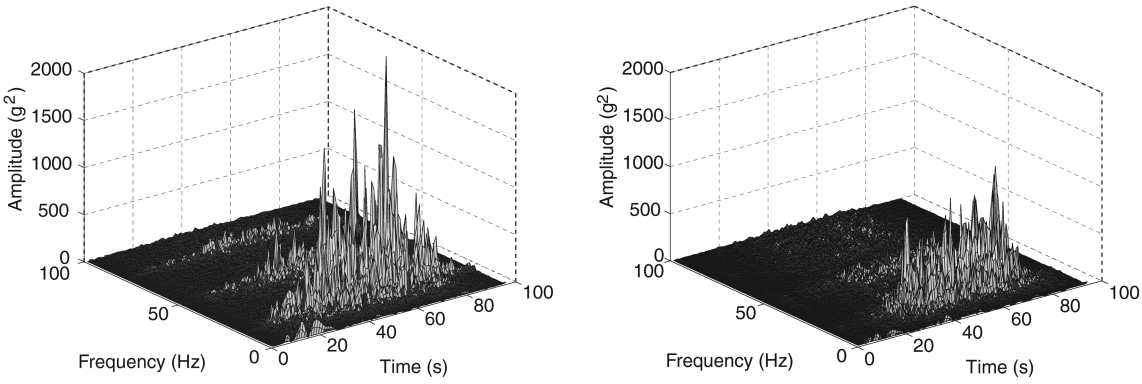

a) No control **b) With control**

Fig. 12 Robust control performance under variable free airflow conditions.

rotating speed of the main motor manually through the console. During the test, the wind-tunnel airflow speed was slowly ramped up from 0–30 m/s, and then ramped down to 0 m/s within approximately 90 s. Because of the broad speed range, the vortex generator was not used to avoid excessive responses of the smart fin. The control law was kept on throughout the test process. Effective and consistent suppression of smart fin vibration responses was obtained. Typical control results are shown in Fig. 12 as waterfall plots.

By comparing the two waterfall plots it was clearly shown that the robust control law functioned well and maintained stable under varying freestream airflow conditions. The smart fin vibration due to varying airflows was suppressed effectively. All three targeted vibration modes have been reduced significantly. On average, the first bending mode decreased by approximately 6.3 dB, the first torsional mode decreased by 4.4 dB, and the second bending mode decreased by 14.5 dB throughout the variable freestream airflow test. Despite the wide range variation of airflow speed, the control law demonstrated satisfactory robust performance and provided significant buffeting load alleviation performance to the smart fin model.

Conclusions

In the development of aircraft buffeting load alleviation systems, dynamic uncertainties exist in the vertical fin dynamics due to varying airflow speed and AOA change during maneuver flight conditions. Wind-tunnel tests have been conducted on a smart fin model to investigate the impacts of airflow aerodynamics using freestream and vortical airflow disturbances. Extensive wind-tunnel test results revealed that

1) High-speed airflow introduced aerodynamic damping and caused modal frequency shift to the smart fin structural dynamics.

2) The extent of aerodynamic influence to the vertical fin dynamic properties increased with airflow speed and varied with AOA configurations.

3) It is imperative to consider the associated aerodynamic effects in the design of control laws for full-scale aircraft buffet load alleviation systems to ensure that the control law robustness should be maintained within the entire flight envelope.

4) A robust control law development strategy based on the structured singular values synthesis technique has been proposed and experimentally verified for vertical fin buffeting load alleviation applications. This provided a feasible strategy of control law development for full-scale aircraft buffeting alleviation systems.

Acknowledgment

The assistance of technical staff from Aerodynamic Laboratory of the Institute for Aerospace Research, National Research Council Canada is gratefully acknowledged.

References

[1] Bretsamter, C., "Aerodynamic Active Control for Fin-Buffet Load Alleviation," *Journal of Aircraft*, Vol. 42, No. 5, 2005, pp. 1252–1262. doi:10.2514/1.8174

[2] Hauch, R. M., Jacobs, J. H., Dima, C., and Ravindra, K., "Reduction of Vertical Tail Buffet Response Using Active Control," *Journal of Aircraft*, Vol. 33, No. 3, 1996, pp. 617–622. doi:10.2514/3.46990

[3] Luber, W., Becker, J., and Sensburg, O., "The Impact of Dynamic Load on the Design of Military Aircraft, Loads and Requirements for Military Aircraft," *IMAC: 16th International Modal Analysis Conference*, Society for Experimental Mechanics, Bethel, CT, 1998.

[4] Sheta, E. F., "Buffet Alleviation of F/A-18 Aircraft Using LEX Fences," *44th AIAA/ASME/ASCE/AHS Structures, Structural Dynamics, and Materials Conference*, AIAA, Reston, VA, April 2003.

[5] Nitzsche, F., Liberatore, S., and Zimcik, D. G., "Theoretical and Experimental Investigations on an Active Control System for Vertical Fin Buffeting Alleviation Using Strain Actuation," *The Aeronautical Journal*, Vol. 105, No. 1047, 2001, pp. 277–285.

[6] Ferman, M. A., Liguore, S. L., Colvin, B. J., and Smith, C. M., "Composite Exoskin Doubler Extends F-15 Vertical Tail Fatigue Life," *34th AIAA Structures, Structural Dynamics, and Materials Conference*, AIAA, Reston, VA, April 1993.

[7] Nitzsche, F., Zimcik, D. G., Ryall, T. G., Moses, R. W., and Henderson, D. A., "Closed-Loop Control Test for Vertical Fin Buffeting Alleviation Using Strain Actuation," *Journal of Guidance, Control, and Dynamics*, Vol. 24, No. 4, 2001, pp. 855–857. doi:10.2514/2.4788

[8] Galea, S. C., Henderson, D. A., Moses, R. W., Zimcik, D. G., White, E. V., and Ryall, T. G., "Next Generation Active Buffet Suppression System," *2003 AIAA/ICAS International Air and Space Symposium and Exposition: The Next 100 Years*, AIAA, Reston, VA, July 2003.

[9] Chen, Y., Wickramasinghe, V., and Zimcik, D. G., "Active Control of a Hybrid Actuation System for Aircraft Vertical Fin Buffet Load Alleviation," *Aeronautical Journal*, Vol. 110, No. 1107, 2006, pp. 315–326.

[10] Chen, Y., Wickramasinghe, V., and Zimcik, D. G., "Development of Smart Structure Systems for Helicopter Vibration and Noise control," *Transactions of the Canadian Society for Mechanical Engineering*, Vol. 31, No. 1, 2007, pp. 39–56.

[11] Wickramasinghe, V., Chen, Y., and Zimcik, D. G., "Experimental Evaluation of a Full-Scale Advanced Hybrid Buffet Suppression System for the F/A-18 Vertical Tail," *Journal of Aircraft*, Vol. 44, No. 3, 2007, pp. 733–740. doi:10.2514/1.25328

[12] Patil, M. J., and Hodges, D. H., "On the Importance of Aerodynamic and Structural Geometrical Nonlinearities in Aeroelastic Behaviour of High-Aspect-Ratio Wings," *Journal of Fluids and Structures*, Vol. 19, No. 7, 2004, pp. 905–915. doi:10.1016/j.jfluidstructs.2004.04.012

[13] Nalbantoglu, V., Balas, G. J., and Thomson, P., "The Role of Performance Criteria Selection in the Control of Flexible Structures," *AIAA Guidance, Navigation and Control Conferences*, AIAA, Reston, VA, July 1996.

[14] μ-Analysis and Synthesis Toolbox, User's Guide, Ver. 3, Mathworks, 2001.